Summer 6-25-2014

Phase change with local thermal non-equilibrium in a two-phase mixture model

Franz Lindner
Universität der Bundeswehr München

Michael Pfitzner
Universität der Bundeswehr München

Christian Mundt
Universität der Bundeswehr München

Proceedings of the 5th International Conference on Porous Media and its Applications in Science and Engineering
ICPM5
June 22-27, 2014, Kona, Hawaii

FLUID FLOW WITH PHASE CHANGE IN VERTICAL POROUS CHANNELS WITH LOCAL THERMAL NON-EQUILIBRIUM IN A TWO-PHASE MIXTURE MODEL

Franz Lindner
Universität der Bundeswehr München, Neubiberg, 85577, Germany, franz.lindner@unibw.de

Michael Pfitzner and Christian Mundt
Universität der Bundeswehr München, Neubiberg, 85577, Germany

ABSTRACT
CFD solutions of multi-phase, single-component flow through a vertical channel, filled with a porous medium, heated from one side, are shown. Steady-state solutions are presented for Darcian flow through capillary porous media. Local thermal non- equilibrium is used with a two-phase mixture. The effects of variation of Peclet-number and dimensionless heat input are shown. The displacement effect of the super-heated vapor reduces the free cross-section of flow of the liquid fluid and accelerates the liquid fluid flowing past the evaporation front. The temperatures, liquid saturations, liquid and vapor heat transfer coefficients are shown for cases with super-heated vapor.

INTRODUCTION
In the literature, the choice of local thermal equilibrium (LTE) or non-equilibrium (LTNE) for numerical models has been discussed for parameters for gaseous fluids [9]. Even without sources or sinks, the fluid mass flow rate (i.e. Peclet number) and the Biot number in the pores are the most important parameters to decide, whether LTE or LTNE should be chosen. Especially for small Biot numbers or high Reynolds-numbers, LTE introduces a large error.
Considering phase change, the small or zero temperature gradient in the fluid within the two-phase zone would act as an artificial insulation zone preventing heat conduction when using LTE. The two-phase mixture model (TPMM) shown here, is an extension of the work by Shi and Wang (2011) for two-dimensional domains and is based on the publications of Wang and Beckermann (1993) and Wang and Cheng (1996). Using a mixture formulation, our model consists only of a small set of conservation equations resembling the set of equations for single-phase flow. Since the mixture formulation does not need to track phase boundaries, the numerical cost is low, however, keeping of course the same physical background as the full separate phase models.
Solutions for a test case similar to Li et al. (2010) are shown for a vertical porous channel, heated from one side. We vary boundary conditions and discuss the effect of changing the dimensionless mass flow rate and the dimensionless heat input.

NOMENCLATURE

Latin Symbols

Bi	=	Biot-number, $\frac{\bar{h}_{sl,in} \cdot D}{\varepsilon \cdot k_s}$
c_p	=	Isobaric specific heat
D	=	Characteristic Length of Porous Medium
f	=	Hindrance function
$\boldsymbol{g}$	=	Gravity vector
Δh_{fg}	=	heat of evaporation
H	=	Enthalpy
$\bar{h}_{si}$	=	Mean heat transfer coefficient between solid and phase i
k	=	Heat conductivity
$\boldsymbol{K}$	=	Permeability tensor
L	=	Length of channel
l_1, l_2	=	Lengths of unheated wall
p	=	Pressure
Pe	=	Peclet-number
$\dot{q}$	=	Heat flux
Ra	=	Rayleigh-number, $\frac{K \cdot g \cdot \rho_l \cdot c_{pl} \cdot W}{\nu_l \cdot k_{f,eff,in}}$
s	=	Liquid saturation
St_v	=	Porous Stanton number of evaporation
T	=	Temperature
$\boldsymbol{u}$	=	Velocity vector, (u, v)

W	=	Width of channel
x, y	=	Coordinates

Greek Symbols

α	=	Thermal diffusion coefficient
ε	=	Porosity
γ_h	=	Advection correction coefficient
Γ_h	=	Effective diffusion coefficient
μ	=	Dynamic viscosity
ν	=	Kinematic viscosity
ρ	=	Density

Subscripts

f	=	Fluid
i	=	Phase i
k	=	Kinetic
l	=	Liquid
s	=	Solid
v	=	Vapor
dry	=	At dryout state
eff	=	Effective
in	=	Inlet
out	=	Outlet

1 MATHEMATICAL FORMULATION

The equations, mixture variables and constitutive relationships proposed by Shi and Wang (2011) are used here. The set of conservation equations is shown in Table 1. Note that variables without a subscript are mixture variables and have to be computed according to the phase state. For definition of mixture variables see Wang and Beckermann (1993).

Table 1: Conservation equations for TPMM with LTNE

Conservation of mass	$\nabla \cdot (\rho \boldsymbol{u}) = 0$
Conservation of momentum	$\boldsymbol{u} = -\frac{\boldsymbol{K}}{\mu}[\nabla p - \rho_k \cdot \boldsymbol{g}]$
Conservation of fluid energy	$\nabla \cdot (\gamma_h \cdot \boldsymbol{u} \cdot H) = \nabla \cdot (\Gamma_h \nabla H) + \nabla \cdot \left[f(\mathrm{s}) \frac{\boldsymbol{K} \cdot \rho \cdot h_{fg}}{\nu_v} \cdot \boldsymbol{g} \right] + \dot{q}_{sf}$
Conservation of solid energy	$\nabla \cdot (k_{s,eff} \nabla T_s) = \dot{q}_{sf}$

1.1 Problem description

We use the same problem as Li et al. (2010) for aiding flow, see Figure 1. Water is flowing through a two-dimensional vertical channel, filled with a porous medium. On one side of the channel, there is a heat source with constant heat flux. The channel width W is 20mm, the channel length L is $8W$, the lengths l_1 and l_2 are both $3W$. Porosity $\varepsilon = 0.75$ as well as permeability of the channel is uniform. All other sides of the channel are adiabatic. Water is entering the channel sub-cooled at a given inlet velocity. At the exit, there is a given pressure boundary condition. The problem is considered to be one-component (water), multi-phase (liquid, two-phase, super-heated) flow with phase-change. Local thermal non-equilibrium of the solid matrix and the fluid is considered.

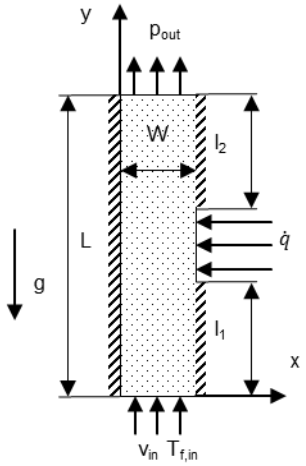

Figure 1: Schematic of the posed problem and boundary conditions for aiding flow

1.2 Boundary Conditions

Boundary conditions are chosen according to Li et al. (2010). Dirichlet boundary conditions for pressure at the outlet p_{out}, and for fluid enthalpy at the inlet, equal to $T_{f,in}$, are chosen. At the inlet, we use a given constant inlet velocity v_{in}. At the walls, we set the normal velocity component $u = 0$. Furthermore, we use Neumann boundary conditions for the energy equation of solid temperature at the walls. For unheated walls, we assume zero temperature gradient, and for the heated section of the wall, we impose a gradient equal to the heat input $\dot{q}$. In addition to this we use a coupled boundary condition for solid energy at the inlet. This is a mixed boundary condition of third order [6]. For fluid energy, we use a Neumann boundary condition with zero gradient for walls and exit, since we consider the fluid to be transparent at the outlet.

2 NUMERICAL SOLUTION

The equation system of Table 1 is solved in an iterative manner in MATLAB with a finite volume scheme. The velocity field is solved using a hybrid solver in MRST v. 2013a [3] with an extension for variable density. We discuss the numerical algorithm and a comparison with results by Shi and Wang (2011) in a companion paper, see Lindner et al. (in preparation). Since phase tracking is not necessary, a staggered grid with uniform cell size is chosen. Grid independency was found for 1280×640 cells, so that the RMS of fluid temperatures between different grids changes less than 0.1%. The convective fluxes are stored at the cell interfaces. The effective diffusion coefficient Γ_h at the cell interfaces is

computed with harmonic mean, which is replaced by arithmetic mean of logarithmic values at the macroscopic phase boundaries since Γ_h degenerates there. Power-Law discretization is used for treatment of the advective and diffusive fluxes for fluid energy. For large advective fluxes at cell interfaces, the numerical scheme is switched to upwind for stability. The Peclet-number at the cells is defined inspired by Patankar (1980) with the cell width Δx and the corresponding velocity component u as

$$Pe^*_x := \frac{\gamma_h \cdot u}{\Gamma_h / \Delta x} \tag{1}$$

The same holds true for cell width Δy and v, respectively. Using this definition, upwind is used at $|Pe^*| \geq 10$. Note that for this distinction, the advective and diffusive fluxes in a mathematical sense, according to tab. 1, are evaluated. In other words, the diffusive fluxes consist of heat conduction and capillary diffusion. Since Pe^* tends to infinity at phase boundaries and is strongly dependent on grid resolution, the choice of numerical scheme plays a role for the solution. Furthermore, in order to evaluate Pe^* at the cell interfaces, γ_h has to be interpolated at the cell interfaces. The same procedure as for Γ_h is used. Due to the coupling of the source term $\dot{q}_{sf}$ to the temperature difference $T_s - T_f$, which is a result of the solution (T_f is an algebraic function of H), the coupled conservation equations have to be solved iteratively:

1. Initialize: $s, T_f, T_s, \boldsymbol{u}$
2. Compute mixture variables
3. Compute velocity field
4. Compute heat transfer coefficients with phase velocities
5. Compute energy field for the coupled energy equations
6. Compute residuum for energy field and continue with 2 if convergence criterion is not met

As a convergence criterion, the RMS of the relative difference of temperatures T_f and T_s between successive iterations should be below 10^{-5}. Under-relaxation iteration is used for the coupled energy equations.

3 RESULTS AND DISCUSSION

The Rayleigh-number according to Li et al. (2010) was set constant to $Ra = 226$. The Biot-Number according to Wang and Wang (2006) was set constant to $Bi = 0.2$. Furthermore, we use dimensionless numbers to characterize the importance of convective heat transport and relative heat input with the Peclet-number [2] and the porous Stanton-number of evaporation, similar to Wang and Wang (2006):

$$Pe := \frac{v_{in} \cdot W}{\alpha} \tag{2}$$

$$St_v := \frac{\int_{l_1}^{L-l_2} \dot{q} dy}{q_{dry} \cdot 2 \cdot W} \tag{3}$$

We chose $\alpha = 0.0033 m^2/s$, see Li et al. (2010). Note that the dryout heat flux is the heat flux which is necessary to completely evaporate the fluid [1].

3.1 Effect of variation of Peclet-number and relative heat input

The influence of convective heat transport and relative heat input is shown by changing Pe and St_v. Figure 2 shows the fluid and solid temperatures as well as the liquid saturation for the case with $Pe = 0.12, St_v = 5.5$ at the wall at $x = W$. Dotted lines indicate the boundary of the heated wall. The temperatures of solid and fluid are almost identical far upstream of the heated wall. Close to the heated wall, the temperatures rise. In the vicinity of the heated wall, the temperature difference is significant and positive at the heated part of the wall and negative downstream of the heated part.
Super-heated vapor is generated near the trailing edge of the heated wall. Further downstream of the heated wall, the temperatures assimilate and re-condensation of fluid takes place.

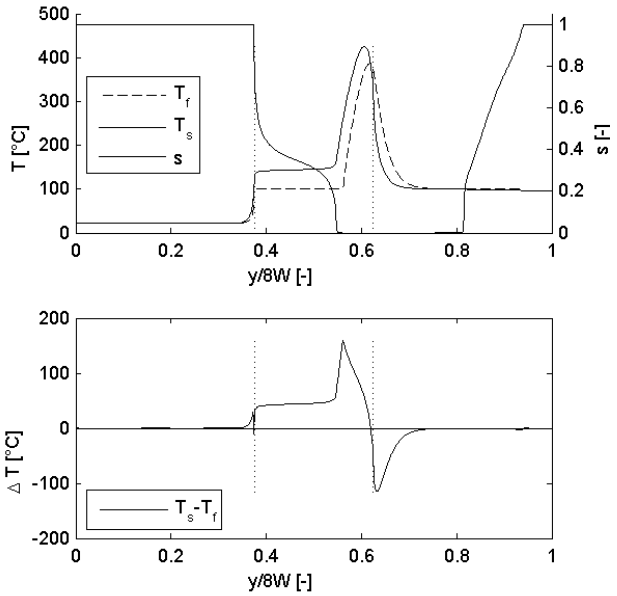

Figure 2: Temperatures, saturation and temperature difference for the case with $Pe = 0.12, St_v = 5.5$.

Figure 3 and Figure 4 show the corresponding liquid and vapor heat transfer coefficients for the case with $Pe = 0.12, St_v = 5.5$. Only certain iso-lines are plotted for better readability. Note that due to the acceleration of the liquid past the evaporation bubble, heat transfer is increased. Inside of the evaporation bubble in the vicinity of the wall, the liquid velocity is low since the vapor

fraction is large. The largest vapor heat transfer coefficients can be found in the vicinity of the super-heated vapor at the trailing edge of the heated wall.

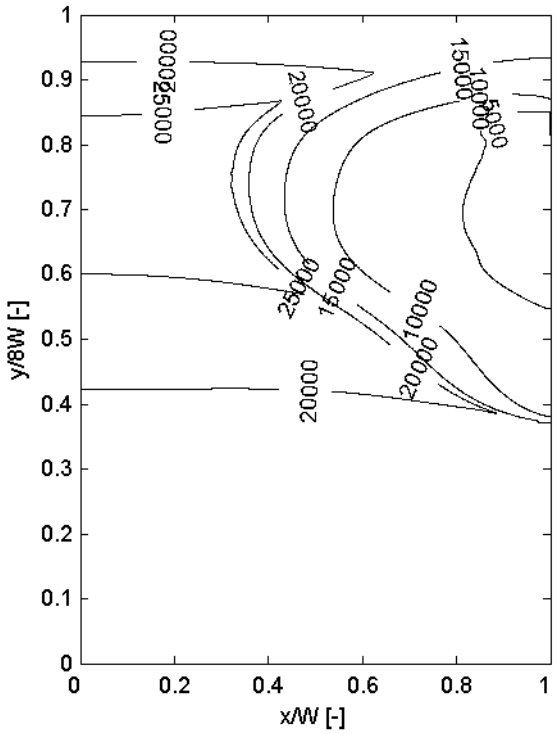

Figure 3: Iso-lines of liquid heat transfer coefficient $\bar{h}_{sl}$ for the case with $Pe = 0.12, St_v = 5.5$. Depicted are only lines with $\bar{h}_{sl} \geq 5000$.

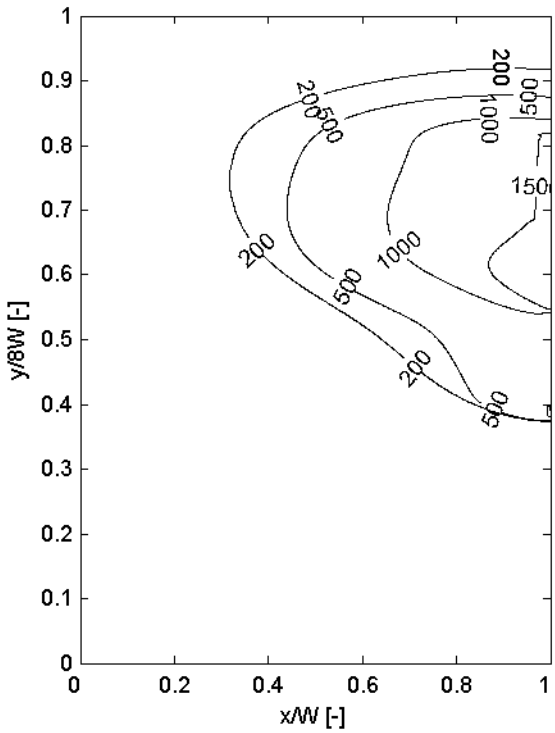

Figure 4: Iso-lines of vapor heat transfer coefficient $\bar{h}_{sv}$ for the case with $Pe = 0.12, St_v = 5.5$. Depicted are only lines with $\bar{h}_{sv} \leq 1500$.

Similar results can be seen for $Pe = 0.06, St_v = 7.5$ in Figure 5, Figure 6 and Figure 7. The region with super-heated vapor is smaller for these boundary conditions. The jumps in the temperature difference indicate the position of the border of the heated wall. A distinctive negative temperature difference between solid and fluid temperature cannot be seen here at the trailing edge of the heated wall, only small to zero temperature differences are present downstream of the heated wall.

Changing the relative heat input, the results can be categorized whether a biphasic or super-heated region is present. For two Peclet-numbers ($Pe = 0.06, Pe = 0.12$), the heat inputs corresponding to the occurrence of a completely liquid domain, of a domain with biphasic flow, and the occurrence of super-heated vapor, have been evaluated. St_v was increased in steps of 0.25 in order to approach the minimal heat input as boundary condition, where super-heated vapor is produced for the first time for this Peclet-number. These cases are accordingly marked in Figure 8. It can be seen that for low Peclet-numbers, the occurrence of super-heated vapor takes a large amount of relative heat input. For large Peclet-numbers, convection is dominating and the heat transfer between solid and fluid is strengthened. Thus, the relative heat input necessary to generate super-heated vapor is smaller.

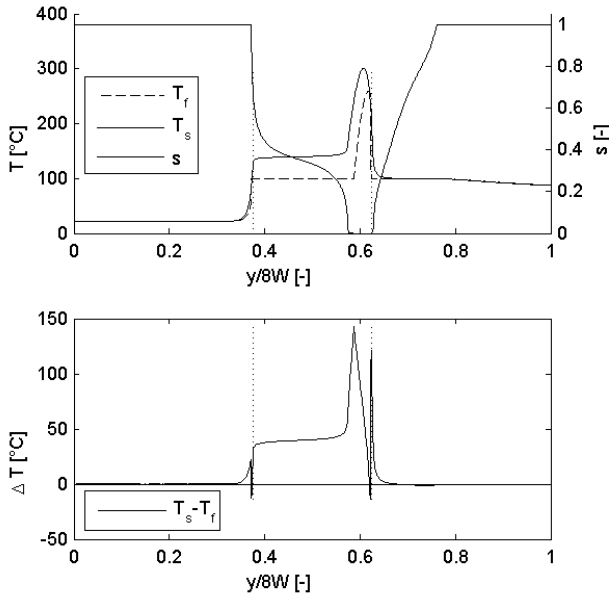

Figure 5: Temperatures, saturation and temperature difference for the case with $Pe = 0.06, St_v = 7.5$.

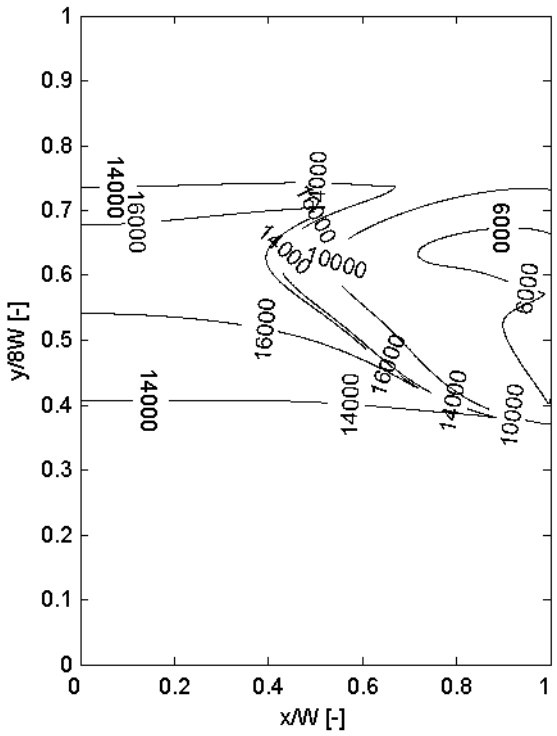

Figure 6: Iso-lines of liquid heat transfer coefficient $\bar{h}_{sl}$ for the case with $Pe = 0.06, St_v = 7.5$. Depicted are only lines with $\bar{h}_{sl} \geq 6000$.

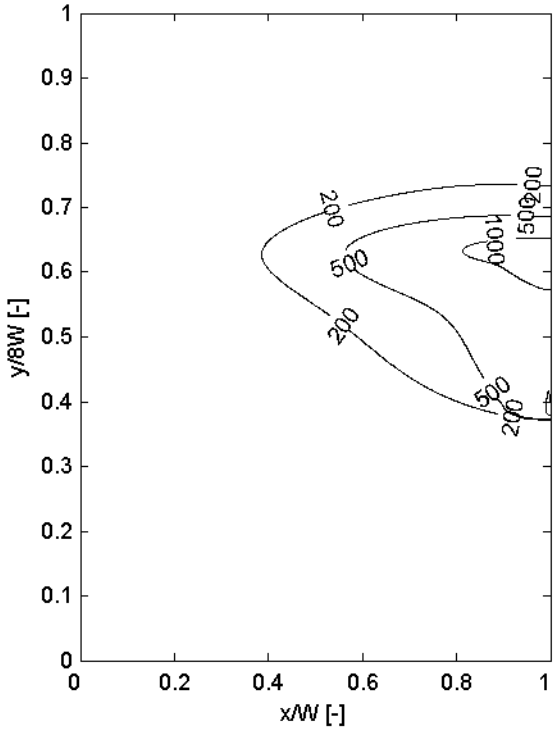

Figure 7: Iso-lines of vapor heat transfer coefficient $\bar{h}_{sv}$ for the case with $Pe = 0.06, St_v = 7.5$. Depicted are only lines with $\bar{h}_{sv} \leq 1000$.

3.2 Reduction of free cross-section for liquid flow by displacement effect of vapor

The generation of super-heated vapor at the heated wall reduces the free cross-section of the liquid fluid and accelerates the liquid fluid flowing past the evaporation front. We define a minimal cross section for liquid fluid $x_{free,l}$ according to the largest prolongation of the biphasic zone lateral to the main direction of flow, i.e. x-direction, for a given set of boundary conditions. This is a measure for the necessary inlet pressure to provide a given inlet flux of water. Smaller Peclet-numbers tend to need larger relative heat input to generate super-heated vapor. The generated super-heated vapor takes less space on the x-direction for smaller Pe, thus $x_{free,l}$ is larger. The results are marked in Figure 8. However, a general rule for the dependency of $x_{free,l}$ on the Peclet-number is yet to be found, since this is only a small sample size.

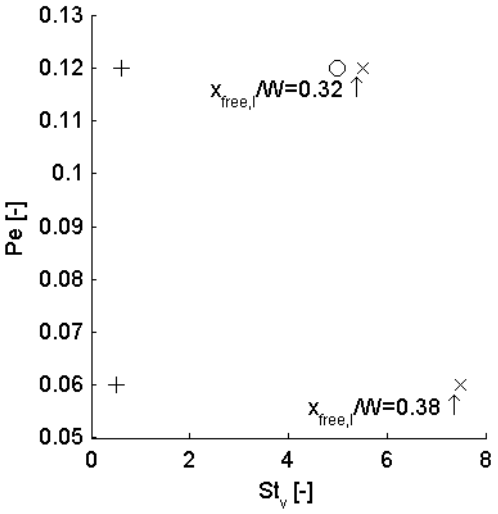

Figure 8: Dependency of phase change on $Pe \& St_v$. Marker $+$ shows that the result only consists of a liquid domain; marker $\circ$ shows that the result has biphasic regions and marker $\times$ shows that super-heated vapor is present in the domain.

4 CONCLUSIONS

We used a two-phase, one-component mixture model with local thermal non-equilibrium to simulate evaporation in a capillary porous media filling a vertical porous channel heated from one side. The influence of inlet mass flow and relative heat input on evaporation has been shown.

We discussed the temperatures and the heat transfer coefficients for both phases. The displacement effect of the super-heated vapor reduces the free cross-section of flow of the liquid fluid and accelerates the liquid fluid flowing past the evaporation front. A trend between the free cross-section of liquid flow and the first appearance of super-heated vapor has been shown.

We are confident with the numerical model for a two-dimensional problem and with the results. Using this model to investigate the dependency of dimensionless characteristic numbers on the evaporation in porous channels is encouraging and we will proceed with a further analysis of the influence of boundary conditions and characteristic numbers on evaporation in local thermal non-equilibrium.

REFERENCES

[1] Kaviany M (1999) Principles of Heat Transfer in Porous Media. (2nd) Springer, Berlin Heidelberg.

[2] Li H, Leong K, Jin L, Chai J (2010) Transient behavior of fluid flow and heat transfer with phase change in vertical porous channels. International Journal of Heat and Mass Transfer. 53: 5209–5222.

[3] Lie KA, Krogstad S, Ligaarden IS, Natvig JR, Nilsen HM, Skaflestad B (2012) Open Source MATLAB implementation of consistent discretisations on complex grids. Computational Geosciences. 16: 297–322.

[4] Lindner F, Nuske P, Helmig R, Mundt Ch, Pfitzner M (2014) Transpiration cooling with local thermal non-equilibrium: Model comparison in multiphase flow in porous media. Transport in Porous Media (in preparation).

[5] Patankar S (1980) Numerical heat transfer and fluid flow. In: Series in computational methods in mechanics and thermal sciences. Taylor & Francis.

[6] Shi J, Wang J (2011) A numerical investigation of transpiration cooling with liquid coolant phase change. Transport in Porous Media. 87: 703–716.

[7] Wang CY, Beckermann C (1993) A two-phase mixture model of liquid-gas flow and heat transfer in capillary porous media - I. Formulation. International Journal of Heat and Mass Transfer. 36: 2747–2758.

[8] Wang CY, Cheng P (1996) A multiphase mixture model for multiphase, multicomponent transport in capillary porous media. part I: Model development. International Journal of Heat and Mass Transfer. 39: 3607–3618.

[9] Wang JH, Wang HN (2006) A Discussion of Transpiration cooling problems through an Analytical Solution of Local Thermal Nonequilibrium Model. Journal of Heat Transfer. 128: 1093-1098.